Wind and Structures, Vol. 8, No. 5 (2005) 325-342
DOI: http://dx.doi.org/10.12989/was.2005.8.5.325

Shielding effects and buckling of steel tanks in tandem arrays under wind pressures

Genock Portela†

General Engineering Department, University of Puerto Rico, Mayagüez, Puerto Rico 00681-9044, USA

Luis A. Godoy‡

Civil Infrastructure Research Center, Department of Civil Engineering and Surveying, University of Puerto Rico, Mayagüez, Puerto Rico 00681-9041, USA

(Received September 14, 2004, Accepted April 20, 2005)

Abstract. This paper deals with the buckling behavior of thin-walled aboveground tanks under wind load. In order to do that, the wind pressures are obtained by means of wind-tunnel experiments, while the structural non linear response is computed by means of a finite element discretization of the tank. Wind-tunnel models were constructed and tested to evaluate group effects in tandem configurations, i.e. one or two tanks shielding an instrumented tank. Pressures on the roof and on the cylindrical part were measured by pressure taps. The geometry of the target tank is similar in relative dimensions to typical tanks found in oil storage facilities, and several group configurations were tested with blocking tanks of different sizes and different separation between the target tank and those blocking it. The experimental results show changes in the pressure distributions around the circumference of the tank for half diameter spacing, with respect to an isolated tank with similar dimensions. Moreover, when the front tank of the tandem array has a height smaller than the target tank, increments in the windward pressures were measured. From the computational analysis, it seems that the additional stiffness provided by the roof prevents reductions in the buckling load for cases even when increments in pressures develop in the top region of the cylinder.

Keywords: bifurcation; buckling; finite elements; steel tanks; tank farms; wind pressures; wind-tunnel.

1. Introduction

This paper reports results of an experimental/computational research program aimed to evaluate the buckling behavior of aboveground short tanks in tank farms under wind loading. Aboveground steel tanks are arranged in various configurations in tank farms, depending mostly on land space. Tandem arrays are commonly found with differences in the location and the distance between the tanks. For tanks located in tandem arrays, designers frequently assume that there are reductions in the wind pressures of the second and subsequent tanks in a row due to shielding effects, but find it difficult to quantify such reductions. There are two main questions opened in this field, first about the pressures acting on tanks which are part of a group, and second, the buckling of the structure

† Assistant Professor, E-mail: gportela@uprm.edu
‡ Professor and Director, E-mail: lgodoy@uprm.edu

under such pressures.

Wind tunnel experiments on silo models in tandem arrays were reported by Esslinger, *et al.* (1971), using slender cylinders with ratio $H/D>1$, where H is the height of the cylinder and D is the diameter. Studies concerning wind pressure distributions measured in circular stacks ($H/D>10$) in tandem arrays and large spacing ($S>D$) have been summarized by Zdravkovich (1977) and Tsutsui, *et al.* (1997). The interference effects using other cylindrical arrays (Gu and Sun 2001) and structures with doubly curvature geometry (Orlando 2001) have also been reported in the literature. However, such geometries are not representative of storage tanks: Low-rise tanks in the Caribbean Region are frequently found with H/D ratios ranging between 0.25 and 0.60 (Virella 2004), and wall to wall separation between tanks in the range of 1/2 D to D.

Thus, there seems to be a void in the technical literature regarding wind pressures in groups of short tanks. Furthermore, the buckling of such tanks as members of a tandem array has not been investigated and only computational buckling results for isolated tanks have been reported. The buckling modes and geometrically nonlinear deformations of slender cylindrical shells under constant wind pressures, with ratio $H/D>5$, have been considered by Greiner and Derler (1993). The buckling of short tanks with open-top has been studied by several researchers (Kundurpi, *et al.* 1975, Flores and Godoy 1998, and Schmidt, *et al.* 1998). Computational models have been extended to investigate the sensitivity of such tanks with respect to geometric imperfections (Godoy and Flores 2002, Jaca and Godoy 2003) as well as the increase in the critical buckling load of the tanks provided by ring-stiffeners (Ressinger and Greiner 1982, Greiner 1998). The methodology used in this paper for the computational analysis of the tanks is similar to those used by Schmidt, *et al.* (1998), Portela and Godoy (2005) in previous studies related to elastic buckling response of cylindrical structures.

A coupled experimental approach in this field would be to simulate the wind flow and the aero-elastic response of the structure in wind tunnel experiments. A more modest approach, followed in this work, is to decouple the flow problem from the structural problem, so that pressures are obtained from the first and are used as an input for the second problem. In the present research, the flow problem is modeled in a small wind tunnel to evaluate pressure distribution, and those are next used in a static nonlinear structural model which is solved by finite element analysis. Specifically, rigid tank models with similar and dissimilar dimensions have been studied in wind tunnel experiments and varying the spacing between them. The buckling behavior of the target tank under the wind pressures obtained in the experiments was next studied by means of bifurcation and geometrically nonlinear analyses.

2. Model set-up in the wind tunnel experiments

Wind tunnel experiments were carried out to obtain the pressure distributions in the cylinder and the roof of a target tank model with conical roof, using one or two other tanks to obstruct the wind flow in a tandem array. The tanks are rigid models constructed in a reduced geometric scale (in the order of 1.18%) with respect to typical dimensions of tanks found in tank farms located in the Caribbean Region (Godoy 1996). The target model was instrumented in order to measure pressure distributions, and either one or two non-instrumented models were used to obstruct the wind flow. In all models, the cylindrical part was made with PVC tubes, while the conical and flat roofs were fabricated with fiberglass.

For the case of two-tank tandem array, the configuration is shown in Fig. 1, in which Tank 1 is the instrumented target tank with conical roof and Tank 2 is the blocking tank with flat roof. H_1 and

H_2 are the height of the shielded tank with conical roof and flat roof, respectively, and S is the wall to wall separation between them. For the tests reported in this section, the models have identical

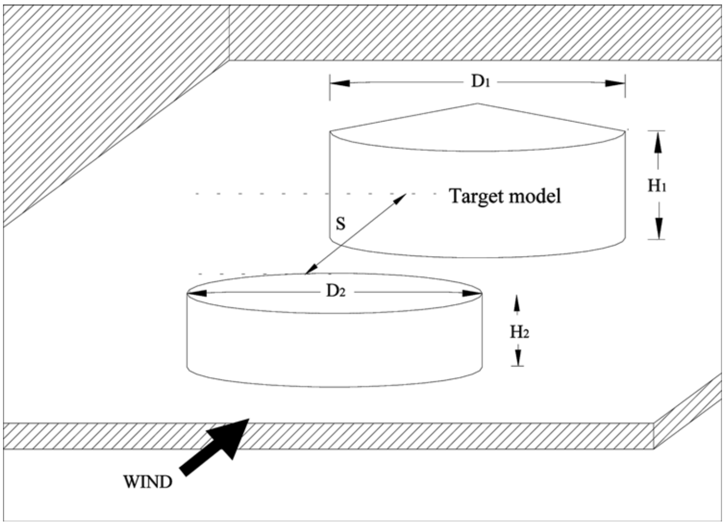

Fig. 1 Tandem arrangement and notation for configurations C1 to C4

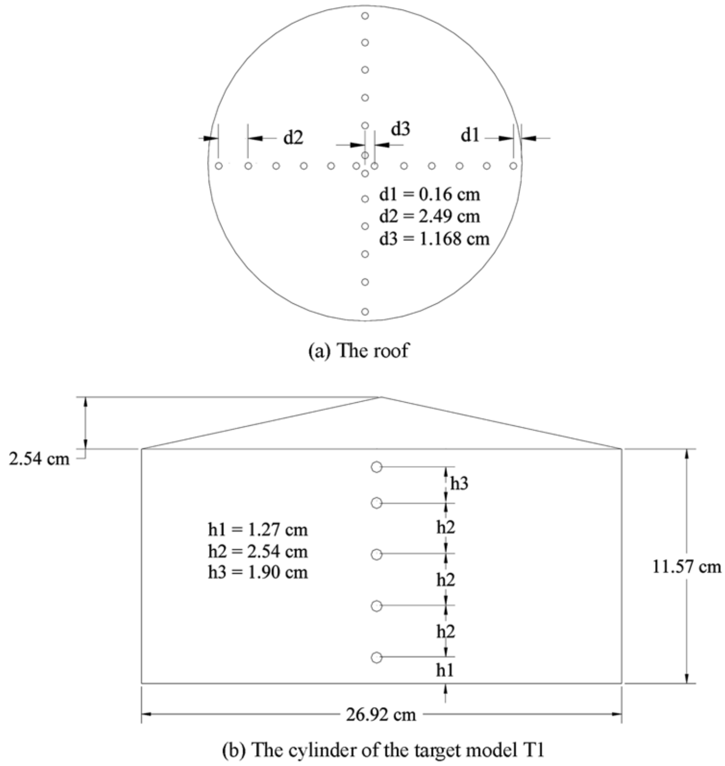

Fig. 2 Location of pressure taps on (a) the roof and (b) the cylinder of the target model T1

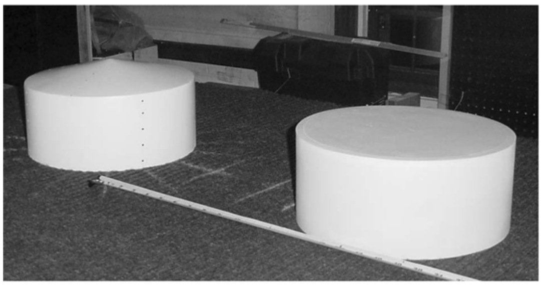

(a) Test C1 (S = 1 D)

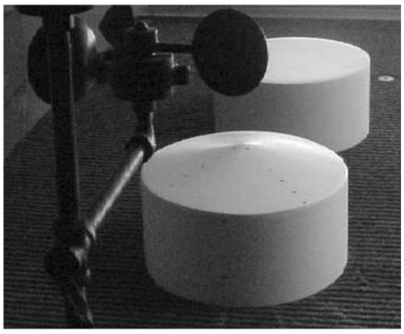

(b) Test C2 (S = 1/2 D)

Fig. 3 Experimental configurations used for (a) Test C1 ($S = 1\ D$) and (b) Test C2 ($S = 1/2\ D$)

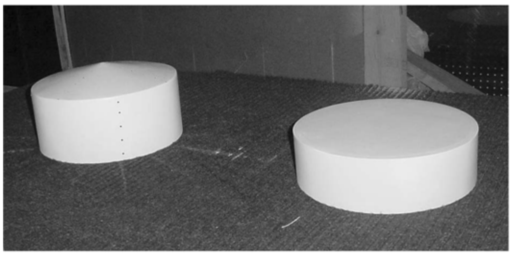

(a) Test C3 (S = 1D)

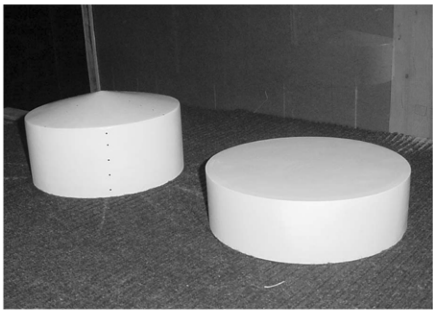

(b) Test C4 (S = 1/2 D)

Fig. 4 Experimental configurations for (a) Test C3 ($S = 1\ D$) and (b) Test C4 ($S = 1/2\ D$)

diameters $D_1 = D_2 = 269.2$ mm. Two geometric parameters were considered to investigate changes in pressure distributions: The height of the cylinder H_1 and the separation distance S between the tanks. The target Tank 1 has a ratio $Hr/H_1 = 0.22$, where Hr is the roof elevation.

The roof was instrumented with 24 pressure taps (6 taps every 90°), and 20 pressure taps (5 taps every 90°) were located on the cylinder, as illustrated in Fig. 2. Several tests were done in which the model was rotated every 22.5°, in order to obtain more complete data around the circumference.

Six configurations were investigated: In the first two cases studied, the two tanks had similar aspect ratios $H_1/D_1 = H_2/D_2 = 0.43$ ($H_1 = H_2 = 115.7$ mm), and the separation between them was $S = D_1$ (case C1) and $S = 1/2\ D_1$ (case C2). The third (C3) and fourth (C4) cases correspond to two tanks with ratios $H_1/D_1 = 0.43$ and $H_2/D_2 = 0.30$, separated at $S = D_1$ and $1/2\ D_1$, and with $H_1 = 115.7$ mm and $H_2 = 81$ mm. The models for test C1 and C2 are presented in Fig. 3, while the set up of tests C3 and C4 are shown in Fig. 4.

Two cases C5 and C6 considering group effects in tandem arrays were also studied, as shown in Fig. 5. The difference in the arrangement of these two tests is the longitudinal distance (S) which separates the target conical roof tank and the two blocking tanks with flat roof. The transverse separation (L) between both blocking tanks was constant ($L = 1/2\ D_2$). Similarly to the previous shielding cases, pressures were measured for the same conical roof tank, since the other tanks were not instrumented. The main features of the blocking models are $H_2/D_2 = 0.39$, with diameter $D_2 =$ 212.7 mm and height $H_2 = 82.6$ mm. For case C5, a distance $S = D_2$ was used, while for tests C6 the

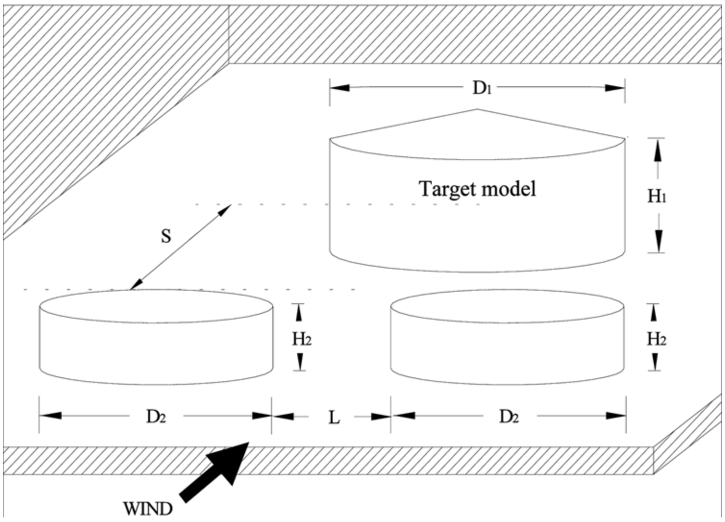

Fig. 5 Tandem arrangement of two tanks with flat roof shielding a tank with conical roof

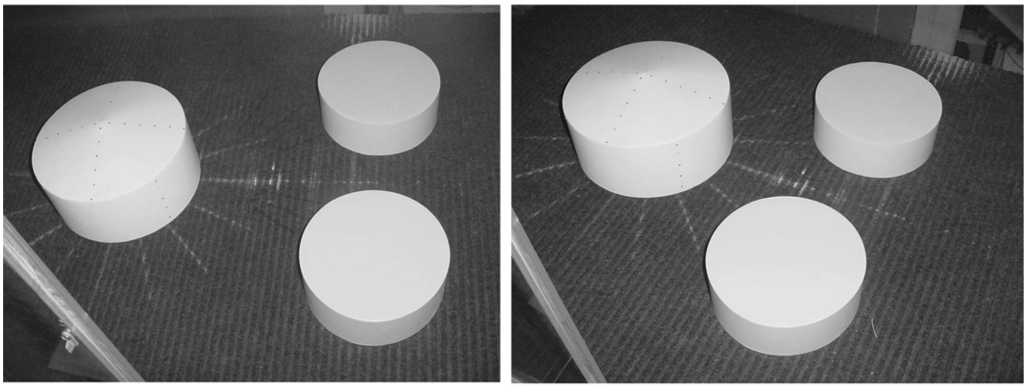

(a) Test C5 (S = 1 D_2) (b) Test C6 (S = 1/2 D_2)

Fig. 6 Experimental setup for (a) Test C5 (S = 1 D_2) and (b) Test C6 (S = 1/2 D_2)

separation was 1/2 D_2. The group arrangements for three models are shown in Fig. 6.

Finally, the target tank was also tested without any blocking tank in front of it to have a reference configuration for an isolated tank and a summary of results is given in Appendix A. A logarithmic mean wind speed configuration was established assuming an open terrain condition with 0.02 m full scale roughness length. The mean pressures were measured at Reynolds number > 2.5×10^5 and are expressed as pressure coefficients (Cp) referenced with respect to the mean wind velocity at a height of 10m from the ground in an equivalent full-scale tank. Full details of the wind tunnel set up are given in Portela (2004).

3. Wind pressure distributions for tandem arrays: A tank with flat roof shielding another tank with conical roof

Fig. 7(a) shows pressure contours measured with the obstacle located at one diameter of separation (case C1). Although the contour pattern is similar to that found for the isolated tank (Appendix A), a considerable decrease in pressure was observed, especially on the wind entrance region to the roof. For this configuration C1, the maximum mean pressures were at the center of the roof. On the windward region, the reduction in suction compared to the isolated tank was 88%, while on the higher zone of the roof the difference was 22% and on the leeward region the difference was 50%.

For the array with one diameter of separation and $H_2\!:\!D_2 = 0.43$ (case C1), the regions with maximum mean pressures and suctions coincide with those of the isolated tanks at angles of 0^o and 90^o, respectively. However, the maximum positive values are located in the higher region of the cylinder (1 *H*) and the values of maximum suction at 0.75 *H*, as illustrated in Fig. 7(b). A reduction in pressure occurs, with the maximum positive and maximum negative coefficients being 30% and 24% lower with respect to the maximum values in the isolated tank.

If the separation is reduced to half diameter (configuration C2, Fig. 8), the reduction of the suctions on the windward region of the roof is more appreciable than for the previous array (C1), and positive pressure values are observed ($Cp = +0.25$). The distribution changes in this region, with a decrease in pressure (changing from positive to negative values) in direction toward the center of the roof. However, from the central region to the leeward of the roof, values exceeding those found in the previous configuration (C1) are observed. As a tank is closer to an obstacle, the pressures tend to decrease, but this is not the case in all the regions of a tank. The maximum mean pressure coefficients are observed at the center of the roof, representing a reduction of 11% with respect to the isolated tank.

Fig. 8(b) shows the pressure contours on the cylinder with half diameter of separation from the blocking tank (case C2). Similar to what was observed in configuration C1, the maximum pressures

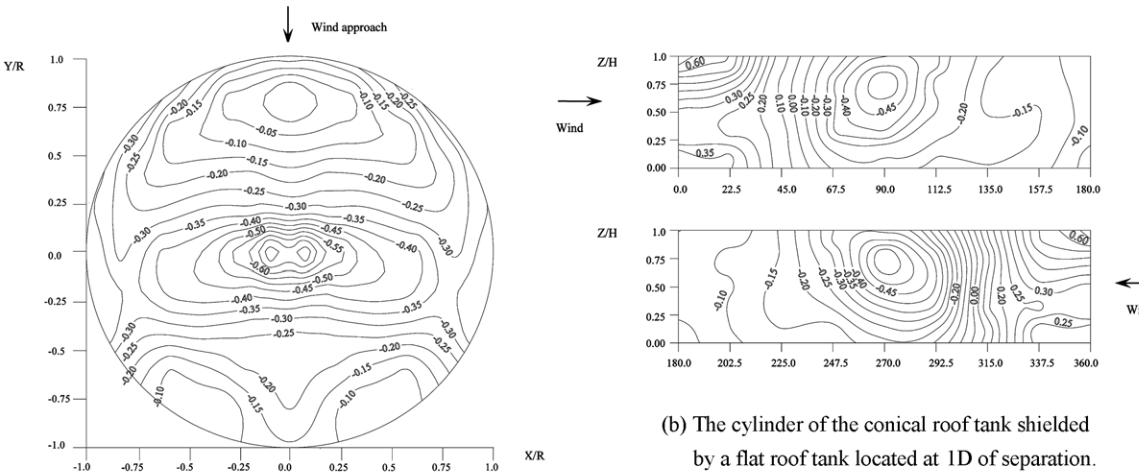

(a) The roof

(b) The cylinder of the conical roof tank shielded by a flat roof tank located at 1D of separation. Hr/D = 0.094, and H_2:D_2 = 0.43

Fig. 7 Pressures for test C1. Mean pressure contours on (a) the roof and (b) The cylinder of the conical roof tank shielded by a flat roof tank located at $1D$ of separation. Hr/D = 0.094, and $H_2\!:\!D_2 = 0.43$

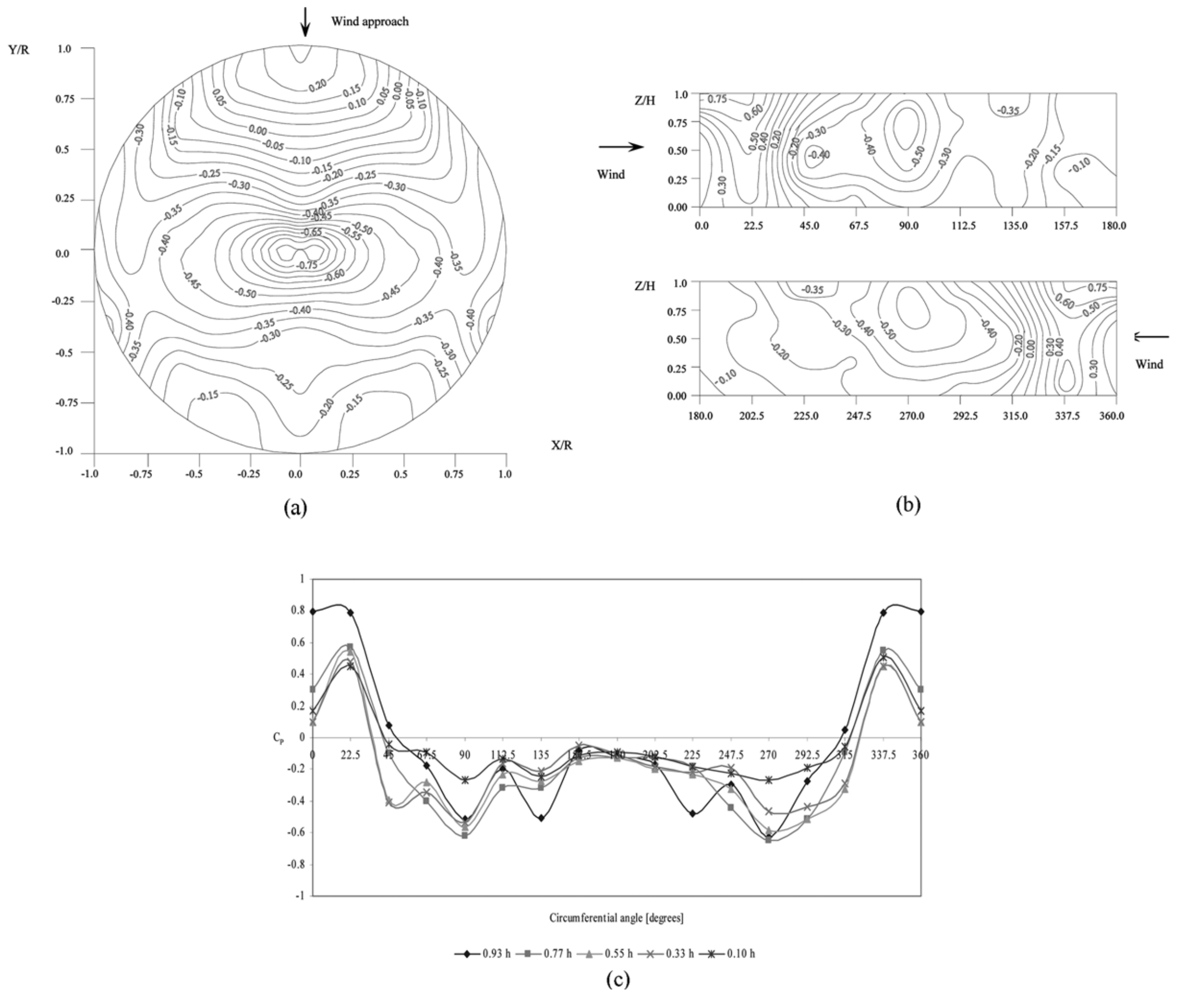

Fig. 8 Pressures for test C2. Mean pressure contours on the conical roof tank shielded by a flat roof tank located at 1/2 D of separation. (a) on the roof, (b) and (c) on the cylinder. $Hr:D = 0.094$, and $H_2:D_2 = 0.43$

(+) develop at a height 1 H and the maximum suctions (−) occur at 0.75 H, referenced from the base of the tank. In certain regions of the cylinder, the maximum pressures and suctions obtained exceed those found with a separation of one diameter. All coefficients at a location of 22.5° from the windward axis show higher pressures than those at 0°, except at a height $H = 0.9$, where a relative constant value is sustained, as presented in Fig. 8(c). A similar behavior was described by Esslinger, *et al.* (1971) in their study of group effects for silos with spherical roofs and ratio $H/D>1$, with a blockage array of 1 D of separation (instead of 1/2 D) and for which the maximum suctions were recorded between 65° and 80° with respect to the windward meridian.

The pressure coefficients obtained on the roof for test C3, representing a configuration of a conical roof tank ($H_1:D_1 = 0.43$) shielded by a flat roof tank ($H_2:D_2 = 0.30$) separated by one diameter, are shown in Fig. 9(a). The pressure coefficients at the entrance have a decrease of 40% in comparison to the isolated case and an increase in the order of 275% with respect to test C1

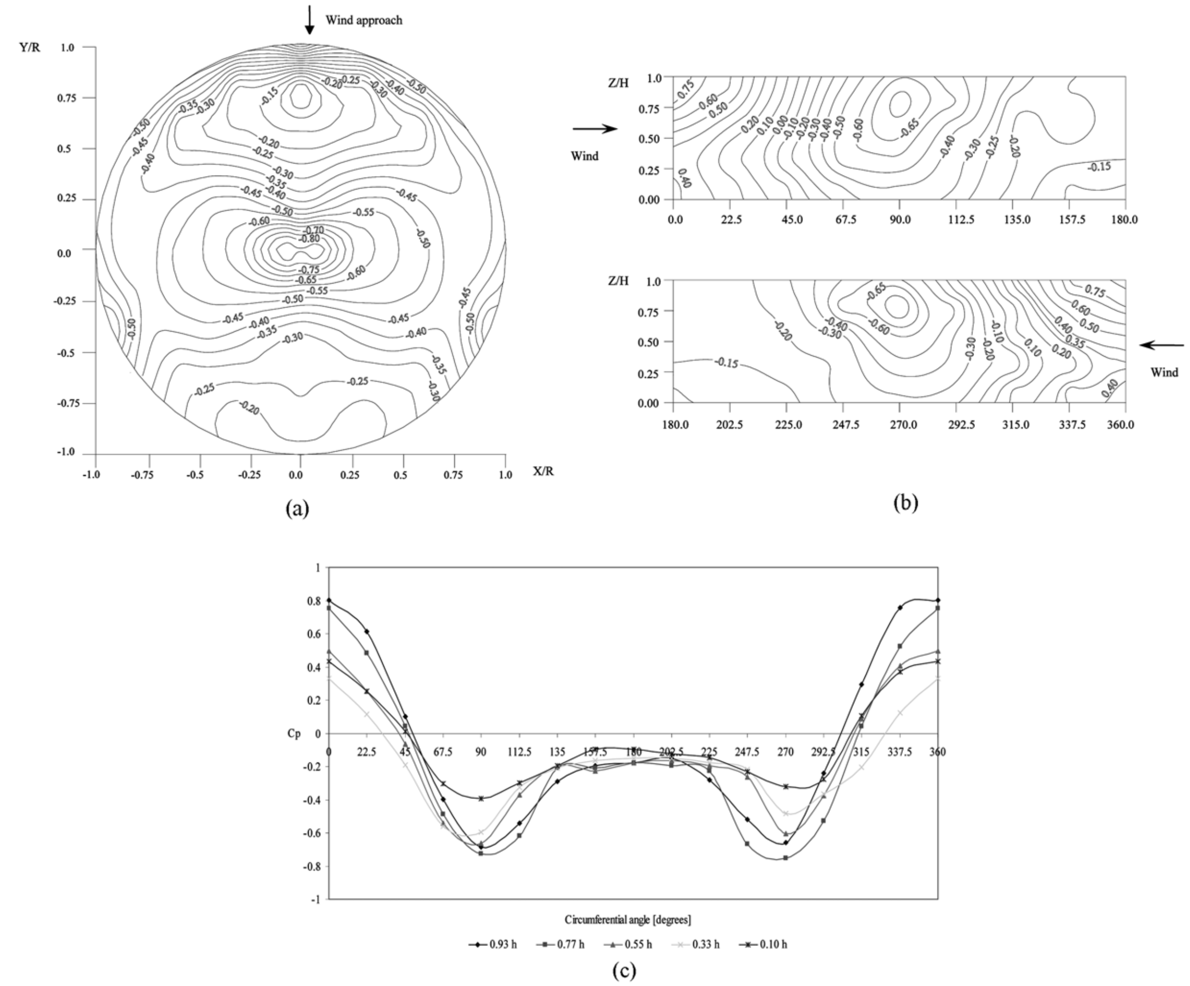

Fig. 9 Pressures for test C3. Mean pressure contours on the conical roof tank shielded by another with similar diameter but lower height. (a) on the roof, (b) and (c) on the cylinder. $Hr/D = 0.094$, $S = 1\ D$, $H_1/D_1 = 0.43$, and $H_2/D_2 = 0.3$

(shielding case with both tanks having similar aspect ratios). The values at the central zone show a small decrease in the order of 6% compared to the pressures in the isolated case and an increase of 18% with respect to test C1.

Fig. 9(b) presents the mean pressure contours measured around the cylinder in test C3. The results show some symmetrical behavior about the windward meridian. The maximum positive pressure coefficients were observed at the windward meridian, with a peak value of $Cp = 0.80$ (Fig. 9(c)), representing a 10% decrease with respect to the isolated case. The most affected region is from 0.80 H to 1.0 H, contrary to the isolated case in which the higher magnitudes were found between 0.5 H to 0.9 H. This behavior was also observed in test C1, but the maximum positive pressure increased by 29% in the present configuration (C3). The maximum suctions were found close to 90° and 270° with a $Cp = -0.75$, representing a small decrease of 9% and an increase of 19% with respect to the

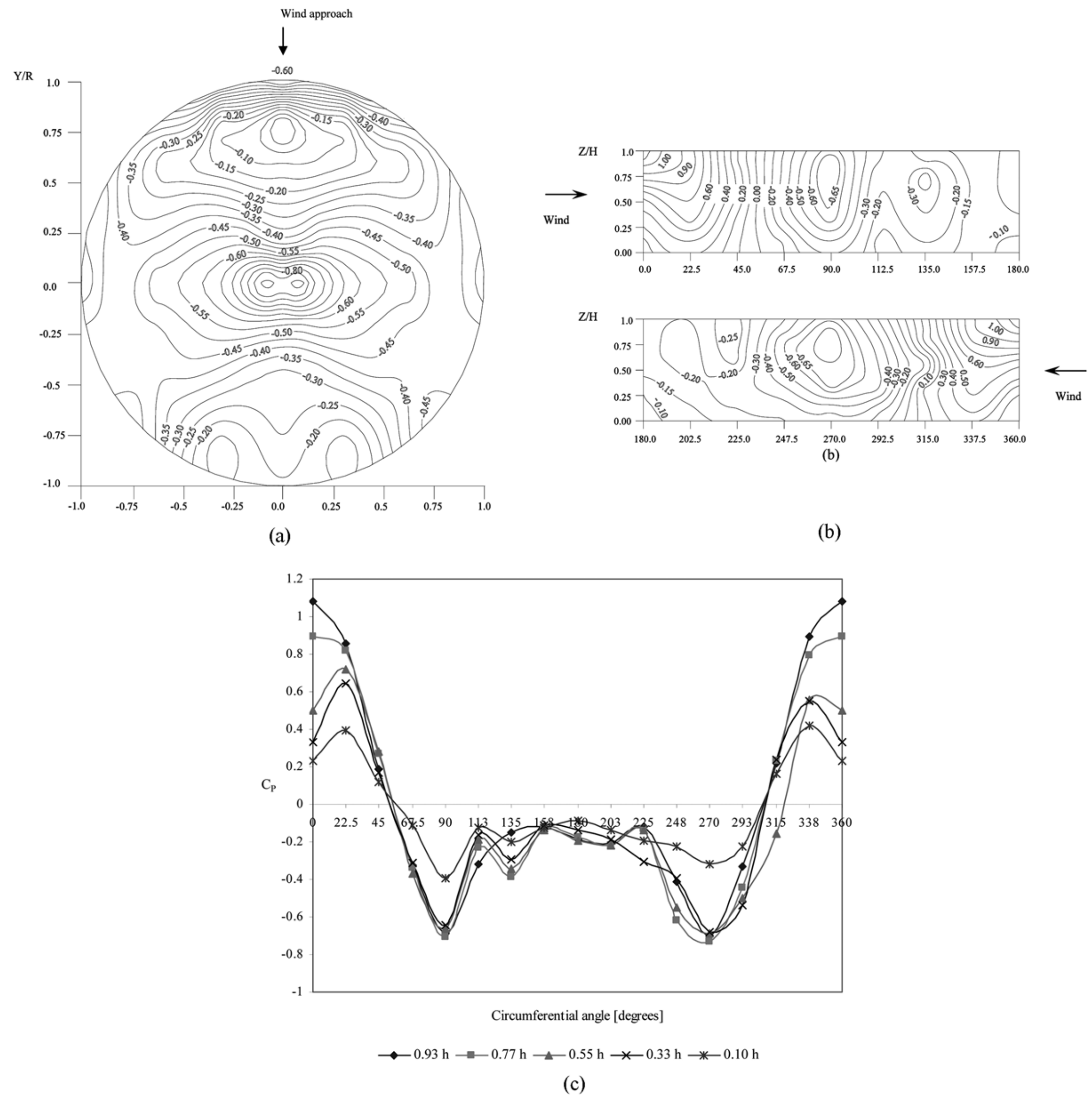

Fig. 10 Pressures for test C4. Mean pressure contours on the conical roof tank shielded by another with similar diameter but lower height. (a) on the roof, (b) and (c) on the cylinder. $Hr/D = 0.094$, $S = 1/2$ D, H_1:$D_1 = 0.43$, and H_2:$D_2 = 0.3$

case of the isolated tank with conical roof and C3, respectively.

The results on the roof of configuration C4 (Fig. 10(a)), consisting of a conical roof tank ($H_1 : D_1 = 0.43$) shielded by a flat roof tank ($H_2 : D_2 = 0.30$) separated by 1/2 D, are very similar to those obtained in test C3, indicating that the difference in separation (S) from D to 1/2 D does not significantly affect the pressure distribution and magnitudes observed on the roof of a higher tank

($H_1 = 115.7$ mm) shielded by a lower tank ($H_2 = 81$ mm). This behavior is different from that observed between tests C1 and C2 (same heights), where the spacing has an influence on the pressures. Unlike the pressures in test C2, all pressure coefficients in C4 were negative on the roof.

Fig. 10(b) presents circumferential distributions for test C4. This case differs from test C2 because of the aspect ratio ($H_2 : D_2 = 0.43$ for case C2). The maximum pressure was found at the highest region of the cylinder on the meridian of wind incidence, with a value of $Cp = 1.08$. This is the highest pressure found among all tests performed. This pressure is 21% and 37% higher than the case of the isolated tank and C2, respectively. In the regions extending from 0° to 22.5° and 360° to 337.5°, an increment in the pressure coefficients was observed at zones of the cylinder below 0.55 H, as shown in Fig. 10(c). This behavior was also observed in test C2, but in this case the increment in pressure occurred in zones below heights corresponding to 0.77 H (Fig. 8(c)).

The difference in height between both configurations affects the spread of this behavior along the height of the cylinder. For test C2 the heights are $H_1 = H_2 = 115.7$ mm, while in test C4, $H_1 = 115.7$ mm and $H_2 = 0.69\ H_1 = 81$ mm. The maximum negative pressures were observed at an angle of 270° with a value of $C_P = -0.73$. Compared to the isolated tank, an 11% decrease is observed; and regarding test C2, an increase in the order of 12% occurred. Similar to what was found in other shielding cases, the values at the leeward region presented coefficients close to $Cp = -0.10$, equivalent to a decrease in the order of 33% in comparison to the isolated tank.

4. Wind pressure distributions for tandem arrays: Two tanks with flat roof shielding another tank with conical roof

For the arrays consisting of two tanks with flat roofs in front of a tank with conical roof (cases C5 and C6), the pressure coefficients measured on the roof of both configurations C5 and C6 with

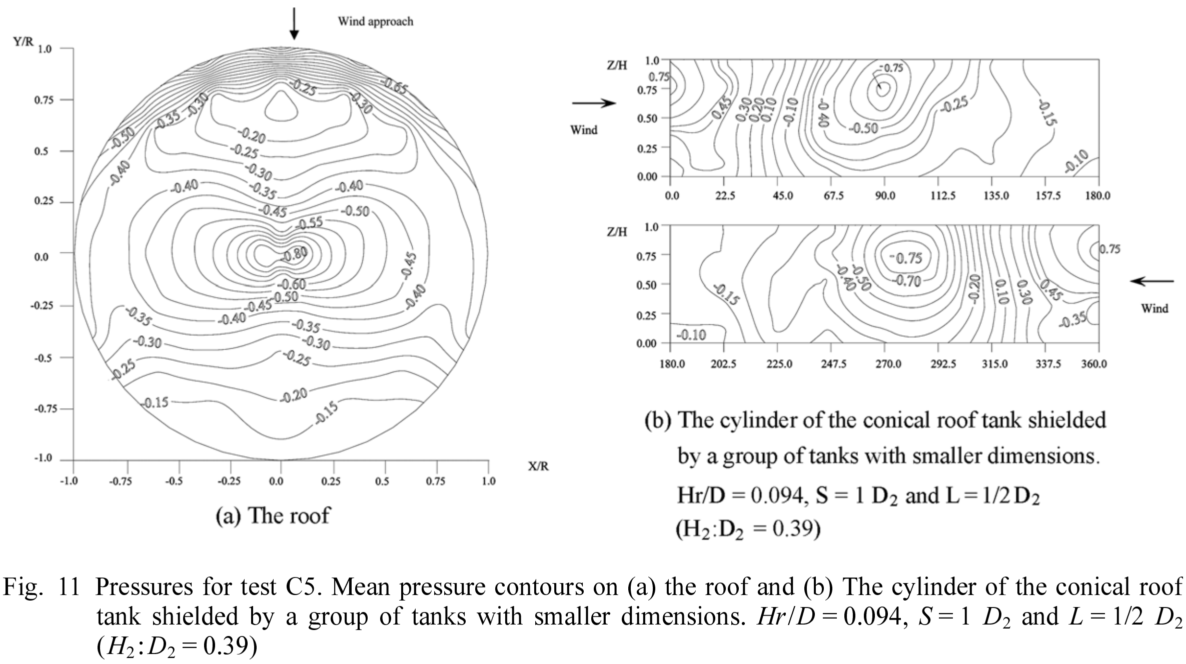

Fig. 11 Pressures for test C5. Mean pressure contours on (a) the roof and (b) The cylinder of the conical roof tank shielded by a group of tanks with smaller dimensions. $Hr/D = 0.094$, $S = 1\ D_2$ and $L = 1/2\ D_2$ ($H_2 : D_2 = 0.39$)

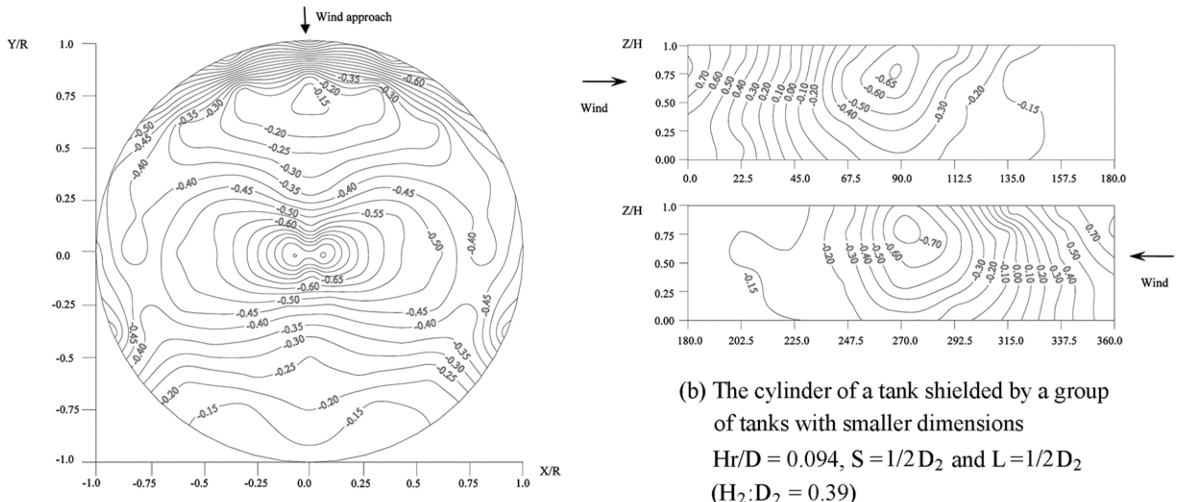

(a) The roof

(b) The cylinder of a tank shielded by a group of tanks with smaller dimensions Hr/D = 0.094, S = 1/2 D_2 and L = 1/2 D_2 (H_2:D_2 = 0.39)

Fig. 12 Pressures for test C6. Mean pressure contours on (a) the roof and (b) the cylinder of a tank shielded by a group of tanks with smaller dimensions. $Hr/D = 0.094$, $S = 1/2\ D_2$ and $L = 1/2\ D_2$ ($H_2{:}D_2 = 0.39$)

$S = D_2$ (C5) and $S = 1/2\ D_2$ (C6) were similar, with maximum suctions at the windward region, as presented in Figs. 11(a) and 12(a). The maximum suctions recorded were $Cp = -1.05$ and $Cp = -1.07$ for tests C5 and C6, respectively. In this entrance region, the values exceed those found in all shielding configurations C1 to C4, but in group arrangements C5 and C6 there is no obstruction in the windward meridian, leading to higher pressures. On the other hand, the resulting pressure coefficients at the center of the roof show small changes in comparison with those obtained in the shielding arrays of tanks with different heights. In this region, the closest configuration (C6) experimented pressures ($Cp = -0.92$) 8% higher than those developed in test T8 ($Cp = -0.85$). At the leeward region, the pressure coefficients were close to −0.15 for both arrangements. The absolute pressure magnitudes recorded in all regions of the roof were smaller in comparison with the isolated case.

The pressure distributions around the cylinder present different patterns between tests C5 ($S = D_2$) and C6 ($S = 1/2\ D_2$), especially at the windward region, but the magnitudes show similarity. In general, the pressures obtained in these grouped tests were lower than those measured in the isolated tank. For both tests C5 and C6 the peak pressures were obtained on the windward meridian at a height of 0.75 H. For test C5, the value of $Cp = +0.79$ was 5% lower than the pressure recorded during test C6 ($C_P = +0.83$), as shown in Figs. 11(b) and 12(b). Peak negative values developed at 90^o and 270^o in test C5 with a $Cp = -0.78$. For test C6, the maximum negative value $Cp = -0.76$ was recorded at 270^o. Similar to the peak positive pressures and for both tests, these values were found at 0.75 H. The pressures observed at the leeward region of the cylinder were in the range of −0.10 to −0.15 for both cases (C5 and C6).

5. Finite element buckling analysis of a tank with conical roof shielded by a tank with flat roof

The buckling behavior of a full-scale tank with dimensions equivalent to the target model studied in the wind tunnel experiments, was next investigated using finite element analysis. Typical heights of these tanks are commonly in a range of 6 m to 20 m, and the diameters vary from 20 m to 40 m. The specific tank investigated has a diameter of 30.48 m, a height of the cylinder $H = 13.11$ m, and a roof elevation $Hr = 2.86$ m, thus having a roof inclination angle of 10.6°. The pressure coefficients were multiplied by a reference pressure $P = 2.45$ KPa (based on ASCE 7-02 Recommendations) and were changed for each case studied (C1 to C6) in order to employ the pressure distributions found in the tests. For the static buckling response, a linear bifurcation approach and a geometric non-linear step-by-step type analysis were performed using the computer program Abaqus (2002). The analyses helped to identify the cases for which a bifurcation analysis may adequately represent the first buckling load and buckling deformation of the tank. These analyses were used to study the variations in the buckling capacity and the buckling modes in shielding configurations. A scale parameter λ was used as the multiplier of the initial pressures considered with which the first buckling pressure of the tank is obtained. The buckling loads are compared with those obtained from the analysis of the isolated tank with conical roof.

The pressure distributions for model C1 are based on a tank shielded by another one of similar dimensions ($H_1 : D_1 = 0.43$) but with a flat roof and located at a distance D_1 in front of it. Fig. 13(a) presents the first mode obtained from an eigenvalue analysis and Fig. 13(b) shows the deflections in the tank from a nonlinear analysis at the first critical point. From the eigenvalue analysis, a wind pressure critical factor of $\lambda = 2.03$ was obtained, practically exceeding twice the value reached for the isolated case and being 4% smaller than the pressure factor computed from the step-by-step analysis ($\lambda = 1.95$). The critical value from the nonlinear analysis is related to a reference wind velocity of 90.5 m/s, and the nonlinear response of the tank follows an unstable behavior, after the critical state, as observed in Fig. 14.

A smaller bifurcation load factor resulted from the shielding configuration separated by 1/2 D (C2), with a value of $\lambda = 1.75$. Similar to the C1 model, and as seen in Fig. 15(a), a higher number of circumferential waves are obtained in comparison to the isolated model, and the maximum modal displacements are not on the windward region of the tank. This behavior was also obtained in the deformed shape reached by the tank at its first critical point with a more realistic nonlinear approach, as presented in Fig. 15(b). This behavior seems to be caused by the shifting (22.5°) observed in the maximum positive pressures developed in the experimental tests (Fig. 8(b)). Moreover, this behavior shows that the pressure pattern has an important influence on buckling mode shapes.

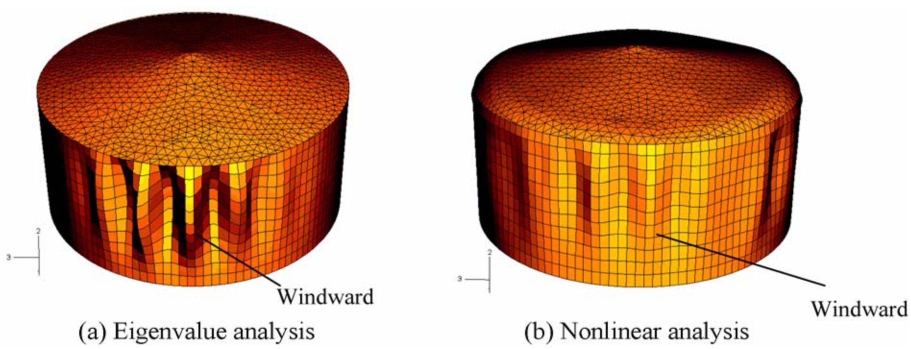

Fig. 13 Mode shapes in model C1 (a) eigenvalue analysis and (b) nonlinear analysis

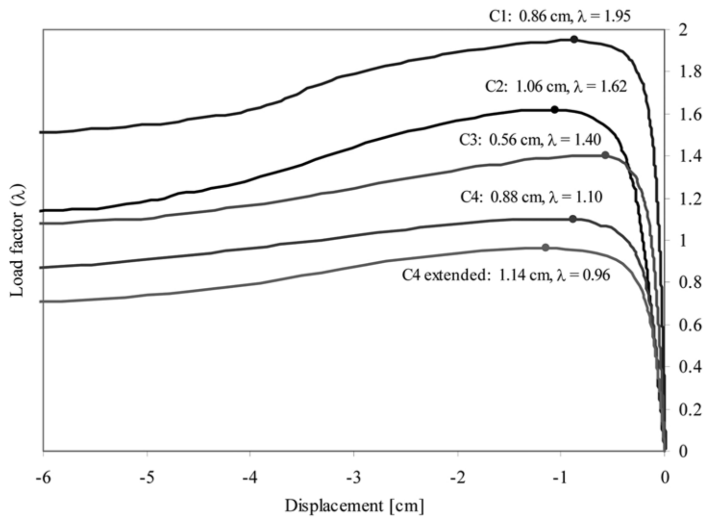

Fig. 14 Load - displacement equilibrium paths for models C1 to C4

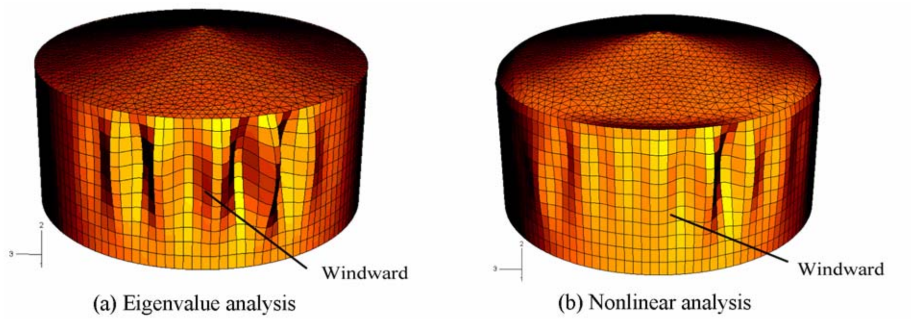

Fig. 15 Buckling mode shapes in model C2 (a) eigenvalue analysis and (b) nonlinear analysis

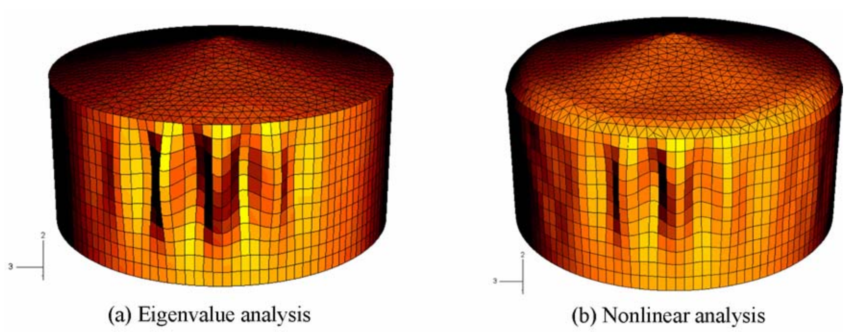

Fig. 16 Buckling mode shapes in model C3 (a) eigenvalue analysis and (b) nonlinear analysis

Fig. 14 depicts the resulting nonlinear response of model C2, for which a pressure factor of $\lambda = 1.62$ was observed, corresponding to a 7.2% reduction in comparison to the eigenvalue analysis. Again, the post-buckling equilibrium path is unstable.

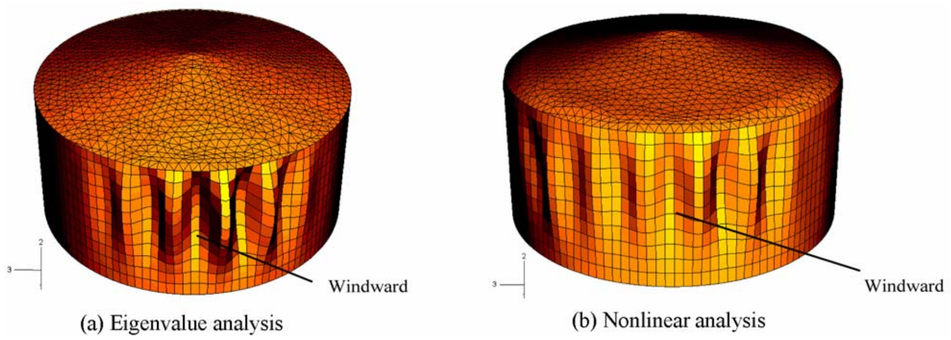

Fig. 17 Buckling mode shapes in model C4 (a) eigenvalue analysis and (b) nonlinear analysis

The first buckling mode shapes in tanks shielded by other tanks with smaller aspect ratios ($H_2:D_2 = 0.3$) are presented in Fig. 16 (C3) and Fig. 17 (C4). The deformed shapes at the first critical point obtained by means of eigenvalue as well as nonlinear analyses are quite similar for the model C3 and for C4. A critical eigenvalue $\lambda = 1.49$ was obtained for model C3 (44% higher than in the isolated tank), while a first critical point with $\lambda = 1.40$ was obtained from the nonlinear path in Fig. 14 (6% smaller than the eigenvalue found from the bifurcation analysis).

Based on the results of the positive pressure coefficients obtained experimentally for this case ($Cp = 0.80$), a lower buckling factor would be expected. However, as observed in the pressure pattern, the maximum experimental positive values developed at elevations between 80% to 100% of the height H of the cylinder, while for the isolated case, the maximum values occur in a region between 50% to 75% H. Apparently, the peak values were near to the cylinder-roof discontinuity in slope which, as observed from the mode shapes, is a very stiff zone of the tank. This behavior was even more evident for model C4, where the maximum positive pressure was found from all the cases studied with $Cp = 1.08$. Again, these pressures are computed in the higher regions of the tank, ranging between 90% to 100% of the height of the cylinder. Contrary to the experimental pressures, the pressure factor from the eigenvalue analysis was $\lambda = 1.19$, which is 15% higher than in the isolated case and 7.6% higher than in the nonlinear results of Fig. 14 ($\lambda = 1.10$). The maximum pressure computed in the nonlinear analysis is related to a reference wind velocity $V = 68$ m/s.

The buckling response of a taller tank was computed to study the influence of the pressures near to the roof (Fig. 18(a)). The diameter and geometry of the tank remains the same, while the height was increased from 13.1 m to 18.3 m ($H/D = 0.60$). New thicknesses were used for the different plates of the shell, as defined by the API 650 recommendations (1991). The pressure contours obtained for the experimental test C4 were extrapolated in the new upper regions of the tank. The eigenvalue is reduced to $\lambda = 1.03$, representing a 13% reduction in comparison to C4 and a value in the same order to that obtained for the isolated model. The nonlinear response of the tank is presented in Fig. 14, where $\lambda = 0.96$ (wind speed $V = 63.5$ m/s). This wind velocity is 2% lower than the reference value used to establish the wind profile. These results suggest that if a lower obstacle is located in front of the tank studied in a tandem configuration, it would develop high external wind pressures at a region far enough from the roof. Under this behavior, the buckling load would be significantly reduced. The buckling mode shapes from the eigenvalue analysis presented in Fig. 18(b) represent well the nonlinear deformations shown in Fig. 18(c),

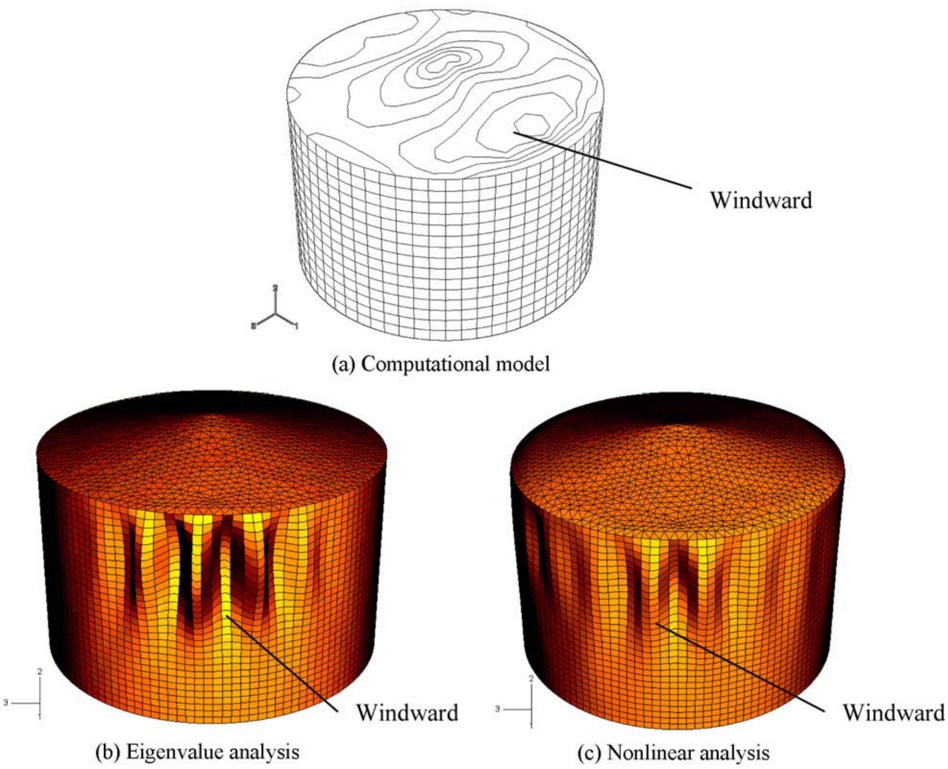

Fig. 18 Tall tank with ratio $H:D = 0.6$ and the pressure distributions obtained for the experimental test C4 (a) computational model, (b) eigenvalue analysis and (c) nonlinear analysis

where it is seen that (contrary to the previous lower tanks studied) the first buckling mode has significant deflections over a zone between 45% to 100% of the height of the tank.

6. Finite element buckling analysis of a tank with conical roof shielded by two tanks with flat roof

For the configuration C5, loaded with the experimental pressures obtained from the group configuration separated at 1.0 D, the bifurcation load was $\lambda = 1.33$, while a $\lambda = 1.296$ was computed for configuration C6 spaced at 1/2 D. Similar buckling modes are also observed, as depicted in Figs. 19(a) and 20(a).

Load factors $\lambda = 1.27$ and $\lambda = 1.16$ were obtained from the nonlinear analysis of configurations C5 and C6 (Fig. 21), which are 4.6% and 10.5% smaller than the resulting eigenvalues for these models. The deformations computed for these tanks (C5 and C6) at the first buckling point, shown in Fig. 19(b) and 20(b), are similar in shape to those computed in the eigenvalue approach, but with more circumferential waves around the cylinder.

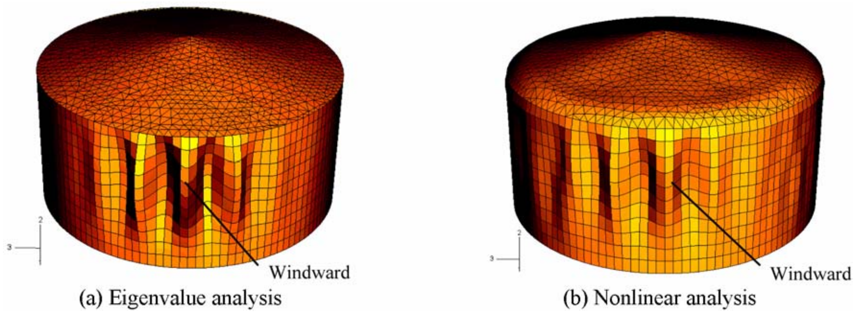

Fig. 19 Buckling mode shapes in model C5 (a) eigenvalue analysis and (b) nonlinear analysis

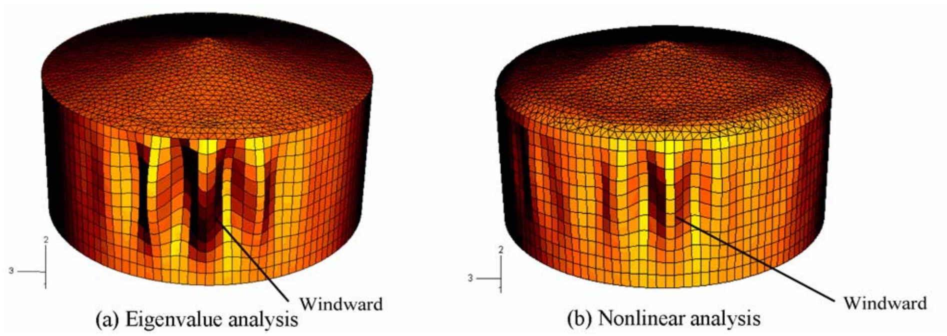

Fig. 20 Buckling mode shapes in model C6 (a) eigenvalue analysis and (b) nonlinear analysis

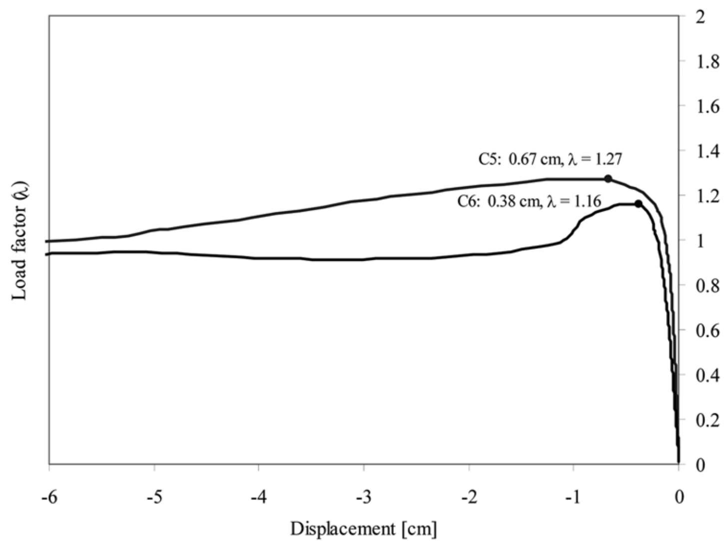

Fig. 21 Load - displacement equilibrium paths for models C5 and C6

7. Conclusions

A tank in front of another tank blocks the flow and can reduce the pressures in some zones of the second tank. However, this effect depends on the relative geometric features and on the separation between the tanks involved. In the worst configuration considered in this paper, with the front tank shorter than the second tank and spaced at 1/2 D, the results show an increase in pressures of the order of 20% and a change in pressure distributions on the windward meridian with respect to the isolated tank.

Group effects are usually responsible for asymmetric distributions of pressures on the cylindrical part of a tank. Furthermore, for close two-tank configurations (i.e. S = 1/2 D) with the same $H:D$ ratio, the largest positive pressures are not coincident with the windward meridian.

For slender tanks with ratio $H:D = 0.6$ (and this may also be applicable to lower obstacles) the critical load is reduced if the maximum positive external pressures acting on the tank are separated enough from the cylinder-roof transition. The results shown in this paper are limited to few tank geometries and group configurations, but they illustrate that tandem configurations with obstacles lower than the blocked tank may induce higher wind pressure patterns and also may reduce the stability capacity of the tank, depending on the location of such high pressures on the height of the cylinder.

Acknowledgements

The authors acknowledge the valuable contribution of Professor Raúl E. Zapata during the experimental part of this research. This research was partially supported by NSF Grant CMS-9907440, FEMA Grant PR0060-A, and the Civil Engineering and Surveying Department of the University of Puerto Rico at Mayagüez.

Appendix A. Wind tunnel pressures and buckling for an isolated tank

The main body of the paper refers to tanks in tandem configuration; however, the results of such

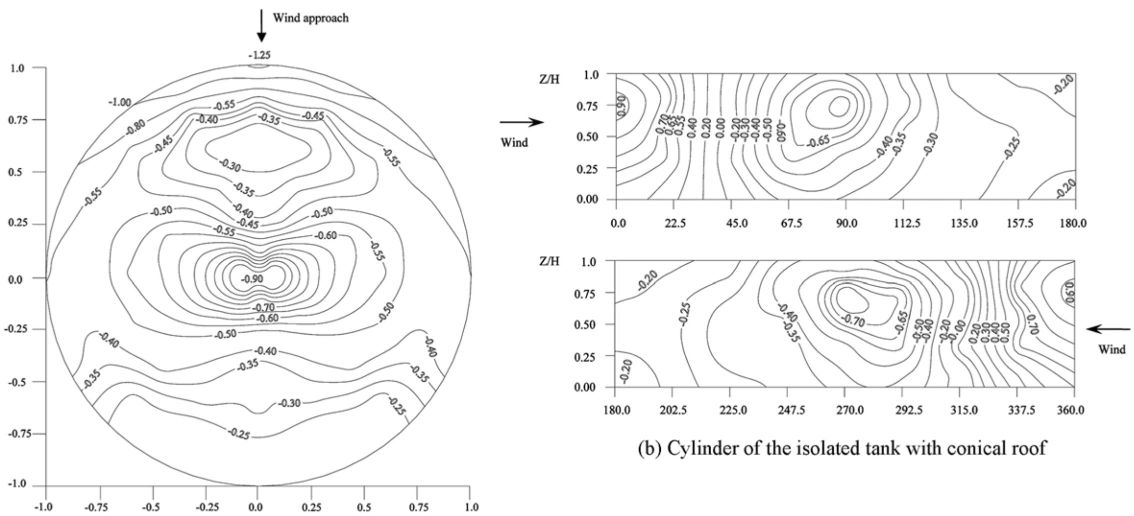

(a) Roof

Fig. 22 Mean pressures on the (a) roof and (b) cylinder of the isolated tank with conical roof configurations are compared with those obtained for an isolated tank to have an idea of changes in pressures and buckling behavior. This appendix shows the pressures obtained in a wind tunnel experiment for just one tank with conical roof, which was later used for the tandem configurations. The results are fully described in Portela (2004). The distribution of pressures is given in Fig. 22.

Buckling studies similar to those reported in Figs. 13~21 were also carried out for the isolated tank. The critical load from the eigenvalue analysis was $\lambda = 1.04$ (Portela 2004).

References

Abaqus (2002), *Abaqus User Manual-version 6.4*. Hibbit, Karlsson and Sorensen Inc., Pawtucket, RI, USA.

API 650 (1991), *Welded Steel Tanks for Oil Storage*, American Petroleum Institute Standard, Chapter 3, Washington, D.C..

ASCE 7 Standard (2002), *Minimum Design Loads for Buildings and Other Structures*, American Society of Civil Engineers, Reston, VA, USA.

Esslinger, M., Ahmed, S. and Schroeder, H. (1971), "Stationary wind loads of open topped and roof-topped cylindrical silos", *Der Stalbau*, pp. 1-8 (in German).

Flores, F.G. and Godoy, L.A. (1998), "Buckling of short tanks due to hurricanes", *Eng. Struct.*, **20**(8), 752-760.

Godoy, L.A. (1996), "Catastrofes produzidas por foracoes no mar do caribe, capitulo 26 in acidentes estruturais na construcao civil", 2 (Ed. A. J. P. da Cunha, N. A. Lima, V. C. M. de Souza), Editora Pini, Sao Paulo, Brasil, 255-262 (in Portuguese).

Godoy, L.A. and Flores, F.G. (2002), "Imperfection sensitivity to elastic buckling of wind loaded open cylindrical tanks", *Struct. Eng. and Mech.*, **13**(5), 533-542.

Greiner, R. (1998), *Cylindrical shells: Wind loading*, Chapter 17 in: Silos (Ed. C. J. Brown and L. Nilssen), EFN Spon, London, pp. 378-399.

Greiner, R. and Derler, P. (1993), *Effect of Imperfections on Wind Loaded Cylindrical Shells*, Institute for Steel and Shell Structures, Technical University of Graz, A-8010, Graz, Austria.

Gu, Z. and Sun, T. (2001), "Classifications of flow pattern on three circular cylinders in equilateral-triangular arrangements", *J. Wind Eng. Ind. Aerodyn.*, **89**, 553-568.

Jaca, R. and Godoy, L.A. (2003), "Colapso de un tanque metálico en construcción bajo la acción del viento", *Revista Internacional de Desastres Naturales, Accidentes e Infraestructura Civil*, **3**(1), 73-83 (in Spanish).

Kundurpi, P.S., Savamedam, G. and Johns, D.J. (1975), "Stability of cantilever shells under wind loads", *J. the Eng. Mech. Div.*, ASCE, **101**(5), 517-530.

Orlando, M. (2001), "Wind-induced interference effects on two adjacent cooling towers", *Eng. Struct.*, **23**, 979-992.

Portela, G. (2004), *Wind Pressures and Buckling of Metal Cantilever Tanks*, Ph.D. Dissertation, University of Puerto Rico at Mayagüez, Puerto Rico.

Portela, G. and Godoy, L.A. (2005), "Wind pressures and buckling of cylindrical steel tanks with a conical roof", *J. Constr. Steel Res.*, **61**, 786-807.

Resinger, F. and Greiner, R. (1982), *Buckling of Wind-loaded Cylindrical Shells - Application to Unstiffened and Ring-stiffened Steel Tanks*, in Buckling of Shells, Ed. Ramn E., Springer, Berlin, 217-281.

Schmidt, H., Binder, B. and Lange, H. (1998), "Postbuckling strength design of open thin-walled cylindrical tanks under wind load", *Thin-Walled Structures*, **31**, 203-220.

Tsutsui, T., Igarashi, T. and Kamemoto, K. (1997), "Interactive flow around two circular cylinders of different diameters at close proximity. Experiment and numerical analysis by vortex method", *J. Wind Eng. Ind. Aerodyn.*, **67**, 279-291.

Virella, J.C. (2004), *Buckling of Tanks Subject to Earthquake Loadings*, Ph.D. Dissertation, University of Puerto Rico at Mayagüez, Puerto Rico.

Zdravkovich, M.M. (1977), "Review of flow interference between two circular cylinders in various arrangements", *ASME J. Fluids Eng.*, **99**(4), 618-632.

CC